VERTICAL TURBULENT BUOYANT HELIUM JET – CFD MODELING AND VALIDATION

Cheng Z[†1], Agranat V.M.[2] and Tchouvelev A.V.[1]
[1]A.V.Tchouvelev & Associates, Inc., 6591 Spinnaker Circle, Mississauga, Ontario, Canada L5W 1R2
[2]Hydrogenics Corp., 5985 McLaughlin Road, Mississauga, Ontario, Canada L5R 1B8

ABSTRACT

In this paper, a vertical turbulent round jet of helium was studied numerically using the PHOENICS software package. The flow was assumed to be steady, incompressible and turbulent. The jet discharge Froude number was 14,000 and the turbulent Schmidt number was 0.7. The incompressible Reynolds average Navier-Stokes equations and helium transport equation expressed in 2-D axisymmetric domain were applied to model the underlying helium release. The k-e RNG turbulence model was used for the calculations of the corresponding turbulent viscosity, diffusivity, velocity and concentration fields in the domain. The simulation results are compared with the experimental measurements from the earlier published studies on helium jets in non-buoyant jet region (NBJ), intermediate region (I) and buoyant plume region (BP). The numerical results show that the radial profiles of mean velocity and mean concentration are consistent with the empirical data scaled by the effective diameter and density-ratio dependence. The mean velocity and concentration fields along the axis of the jet agree with the decay laws correlated from the previous experiments. The discrepancy between the numerical and experimental data is within 10%, proving that the current CFD model for gas release and dispersion is robust, accurate and reliable, and that the CFD technique can be used as an alternative to the experiments with similar helium jets. The authors believe that the current CFD model is well validated through this study and can be further extended to predict similar hydrogen releases and dispersion if the model is properly applied with hydrogen properties.

1.0 INTRODUCTION

The purpose of this research effort is to validate the previously developed CFD models by using the published experimental data for gas releases. Due to the scarcity of reliable published experimental data available for hydrogen releases, experimental helium jet data, obtained by Keagy and Weller [1], Way and Libby [2], Aihara et al. [3], Pitts [4], and Panchapakesan and Lumley [5], were used as an alternative for the current validation. The approach is to compare the non-dimensional velocity and concentration fields predicted by CFD simulations to the empirical data. An axisymmetric vertical helium jet reported by N.R. Panchapakesan and Lumley [5] was used as the benchmark problem for the simulations.

The jet flow field is generally divided into three regions according to the relative strength of buoyancy effects: non-buoyant jet region (NBJ), the intermediate region (IR) and the buoyant plume region (BP) [6]. Survey of helium jet measurements shows several experimental data related to these three regions. Keagy and Weller [1] first used a sampling probe to measure mean concentration and a Pitot probe to measure mean velocity for the helium releasing from a sharp-edged orifice. Their experimental data reflects the physical behaviors in the non-buoyant region (NBJ), which is dominated by strong convection forces. Aihara, Koyanma and Morishita [3], using a hot-wire probe, reported comprehensive measurements in a high-velocity small-diameter jet in the non-buoyant region (NBJ) as well. Way and Libby [2] developed an interference concentration probe and reported limited measurements in a helium jet close to the nozzle in the intermediate region (IR). Using a composite probe consisting of an interference probe of the Way-Libby type and an x-probe, Panchapakesan and Lumley [5] reported extensive measurements of simultaneous values of helium concentration and two velocity components for an axisymmetric helium jet in the intermediate region (IR). Pitts [4] studied a free helium jet in air and measured the concentration field with a laser-induced Rayleigh scattering technique. Chen and Rodi [6], in a review of vertical turbulent buoyant jets, developed the empirical non-dimensional parameters for delineating the three regions (NBJ, IR and BP). The non-

[†] Corresponding author: e-mail address: zcheng@tchouvelev.org

dimensional quantities for velocity, concentration and coordinates were developed using the dimensionless density, length, the Froude number (or the Richardson number) and density ratio. The above findings are used for the present CFD validation.

Previous analysis of similarity between hydrogen and helium done by V. Agranat et al in [7] showed that hydrogen and helium have very similar behavior in non-buoyancy dominant regions. Since this analysis considers the turbulent jets of helium with relatively high Reynolds numbers, it can thus be applied to model validation of similar hydrogen jet releases.

2.0 PROBLEM DEFINITION AND MODELING APPROACH

The CFD simulation of a helium jet exploited the experimental set-up used by Panchapakesan and Lumley [5]. Helium leaked vertically from a round orifice of 6.12 mm diameter at a constant velocity of 72.5 m/s into a room of 4.25 m × 4.25 m × 3.75 m. The corresponding leak rate was 2.13×10^{-3} m^3/s, or 0.356 g/s. The release was assumed to be steady state. A 2-D cylindrical domain of 0.5 m (radius) by 3.0 m (long) was used for this steady-state CFD simulation to save the computational resources. The flow was assumed to be 2-D flow, which was symmetric in the angular direction. The PHOENICS [8] software was used for solving the problem modeled by 2-D Navier-Stokes equations and helium mass transport equation in the spatial coordinates (r, x). Here r and x denote the radial and axial coordinates respectively.

The mixture gas density, ρ, is dependent on the helium mass concentration, C, standard air density, ρ_{air} (ρ_{air} = 1.209 kg/m^3), and helium density, ρ_{He} (ρ_{He} = 0.167 kg/m^3):

$$\frac{1}{\rho} = \frac{C}{\rho_{air}} + \frac{1-C}{\rho_{He}}, \qquad (1)$$

An inverse-linear option for density calculation was set in the PHOENICS interface based on Equation 1.

The effective viscosity was calculated based on laminar viscosity and turbulent viscosity. The laminar viscosity is dependent on the volumetric concentration of helium, the laminar viscosities of helium and air, and the mixture density: $\mu_l = a\mu_{He} + (1-a)\mu_{air}$, where μ_{He} is the laminar viscosity of helium ($\mu_{He} = 1.94\times10^{-5} Ns/m^2$), μ_{air} is the laminar viscosity of air ($\mu_{air} = 1.82\times10^{-5} Ns/m^2$) and a is the volumetric concentration of helium, which can be evaluated by $a = C\rho/\rho_{He}$. The turbulent viscosity was calculated using k-e RNG model [8, 9] (renormalization group k-e turbulence model), which is implemented in the PHOENICS software. The turbulent kinetic energy and its dissipation rate, k and e, were solved using kinetic energy and its dissipation rate transport equations with Prandtl numbers (transport coefficients) of 0.7194 [8, 9]. The turbulent viscosity was generally much larger than the laminar viscosity, so the laminar viscosity could be neglected in turbulent flow regions. But far away from the leak orifice, the flow was laminar and the laminar viscosity was significant. The current approach of the effective viscosity efficiently considered both the laminar and turbulent viscosity contributions in the whole domain and was implemented in the simulation of the current problem.

The effective helium diffusion coefficient in air is the summation of the laminar diffusivity and the turbulent diffusivity. The laminar diffusivity is $5.7\times10^{-5}\ m^2/s$ for helium. As the turbulent Schmidt number was about 0.7 as evaluated by Panchapakesan and Lumley [5], the turbulent diffusivity was assumed to be equal to the turbulent kinematic viscosity divided by 0.7.

The boundary conditions at the leak orifice were set by a user-defined patch with the leak velocity of U_j = 72.5 m/s (velocity in the axial direction) and fixed mass flux of ρU_j =12.151 kg/(m^{2}s). Here, U_j denotes the leak velocity at the jet orifice. The turbulent intensity at the leak orifice was about 0.2% according to the measurement [5]. For simplicity, in the current CFD modeling, it was assumed to be zero at the orifice.

Let $\vec{u} = (u_r, u_x)$ denote the velocity vector. The boundary conditions at the boundaries of the domain excluding leak location were as follows:

k =0, e =0, $\vec{u} = (u_r, u_x) = (0,0)$ and $C = 0$ at (0.5 m, x), (r, 0 m) and (r, 3 m).

3.0 NUMERICAL RESULTS

The numerical simulations were performed on two structured meshes: the coarse mesh was 60×60 with 8 cells for the 3.06 mm radius leak orifice, and the fine mesh was 90×90 with 12 cells for the leak orifice. Power law grid distributions [8] were used for the mesh generation so that the computational region near the leak orifice was divided by relatively fine grids.

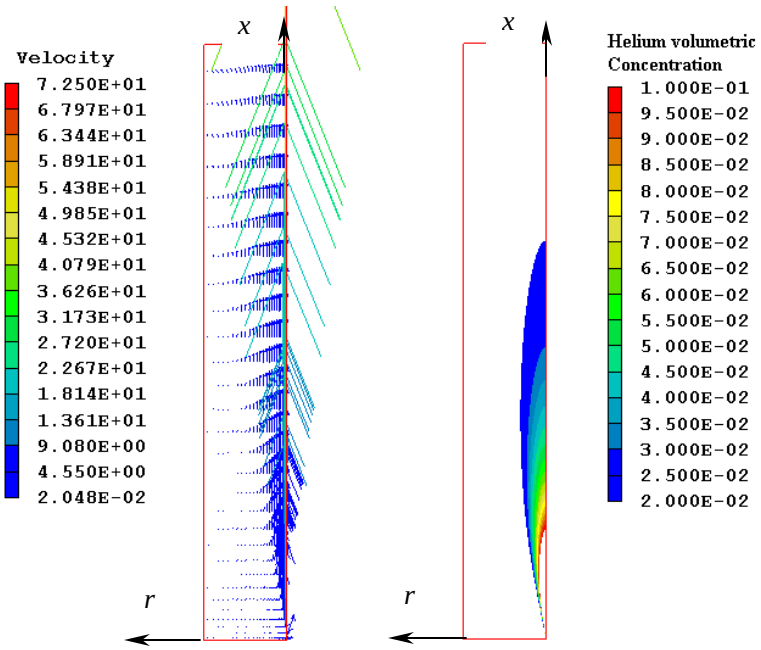

Figure 1. Velocity vectors (left) and volumetric concentration (right) profiles in the (r, x) plane

The computational domain is symmetric in the angular direction.

Figure 1 shows the velocity vectors and helium volumetric concentration profiles obtained on the fine mesh (90×90). In order to show the velocities clearly, the velocity field is plotted by every third velocity vector in the radial and axial directions. The concentration is only shown in the region between 2% to 10% He vol. Sensitivity studies, using the coarse mesh 60×60, showed the similar results, indicating that the current grid density is fine enough to yield reliable simulation results.

Table 1 shows the axial volumetric concentrations and axial velocities (U_s), along the jet centre line, obtained by the experiment [5] and current CFD simulations. The corresponding errors are shown in percentage. As we see, the k-e RNG model successfully predicts the concentration and velocity fields in the turbulent jet flow.

Table 1. Axial mean values of volumetric concentrations and velocities along the jet centre line

$r = 0$	Volumetric concentration			Velocity, U_s		
x (m)	Exp. (%)	CFD (%)	Error (%)	Exp. (m/s)	CFD (m/s)	Error (%)
0.306	18.0	19.3	7.51	3.15	3.36	6.67
0.3672	14.7	15.9	8.15	2.59	2.72	5.02
0.4284	12.6	13.4	6.04	2.27	2.30	1.32
0.4896	11.3	11.5	2.36	2.01	2.00	-0.50
0.5508	10.0	10.1	0.53	1.86	1.78	-4.30
0.612	9.02	8.91	-1.26	1.69	1.61	-4.73
0.6732	8.30	7.94	-4.09	1.58	1.48	-6.33
0.7344	7.68	7.16	-6.63	1.49	1.38	-7.38

Let x/d define the dimensionless quantity corresponding to the relative axial distance to the jet, where d is the diameter of the leak orifice (d=6.12 mm), and let U_j/U_s define the dimensionless quantity corresponding to relative axial mean velocity, where U_s is the axial mean velocities along the jet centreline, namely $U_s = u_x(0, x)$, and U_j is leak velocity at the orifice. The CFD results can be compared to the nonlinear polynomial curve fit and linear fit to Panchakepasan and Lumley's experimental data as shown in Figure 2. The CFD results show a good agreement with the experimental data, which can be correlated as $U_j/U_s = 0.414\ x/d$ [5].

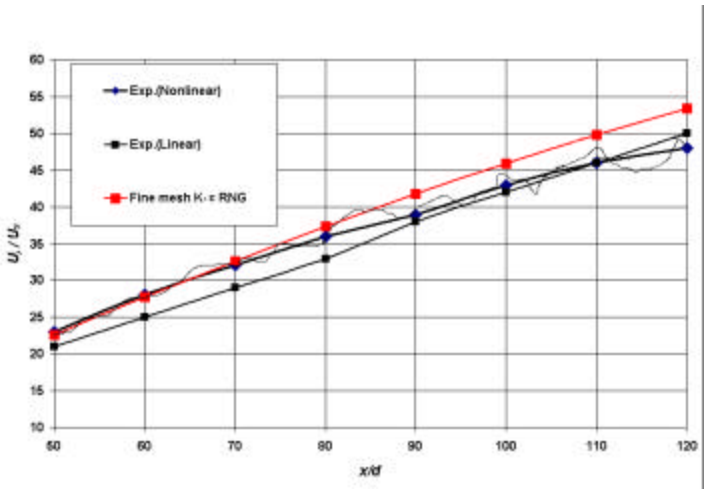

Figure 2. Variation of the dimensionless axial mean velocity U_j/U_s along the jet centreline

The red line marks the CFD results obtained by using k-e RNG model on the fine mesh. The dark blue and black lines show the nonlinear polynomial curve fit and linear fit to Panchapakesan and Lumley's experimental data, respectively.

Similarly, the CFD results for the mean helium mass concentrations at the centreline, $C_s = C(0, x)$, match the linear fit to Panchapakesan and Lumley's mass concentration measurements with $1/C_s = 0.73\ x/d$ [5] as shown in Figure 3. The results also agree perfectly with Pitts' experimental data for a free helium jet [4].

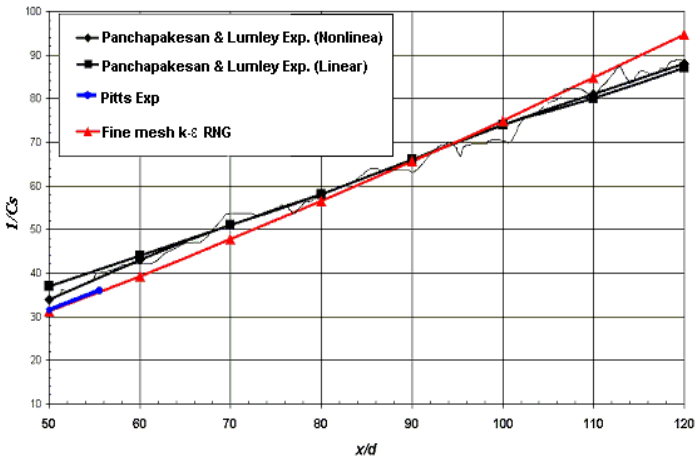

Figure 3. Variation of the mean helium mass concentration C_s along the jet centreline

The red line marks the CFD results obtained by using *k-e* RNG model on the fine mesh. The two black lines mark the nonlinear polynomial curve fit and linear fit to Panchapakesan and Lumley's experimental data. The blue line marks the experimental data from Pitts.

Another important dimensionless quantity is defined as *r/x*, where *r* is the radial distance to the centerline. Figure 4 shows the radial profile of the dimensionless quantity, *U/Us*, which represents variation of the axial mean velocity *U* with the radial distance *r*. Here $U = u_x(r, x)$.

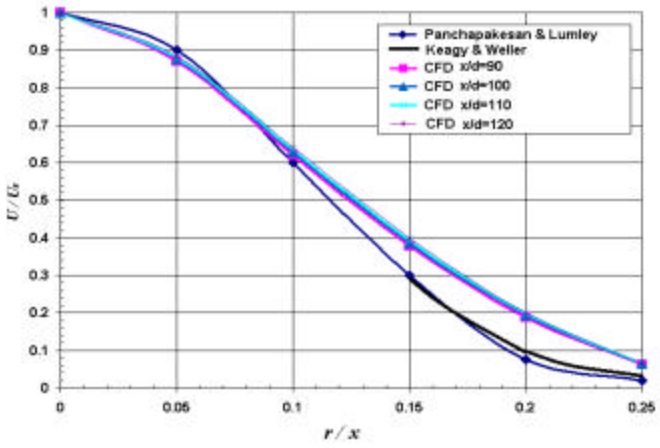

Figure 4. Radial profile of axial mean velocity

The dark blue and black lines mark the correlated Panchapakesan and Lumley's data and Keagy and Weller's data, respectively. The magenta, blue, cyan and purple lines mark the CFD results corresponding to *x/d* =90, 100, 110 and 120, respectively.

Figure 5 shows the radial profile of the dimensionless quantity, C/C_s, or the ratio of the mean helium mass concentration over its centerline value with respect to the radial coordinate. The CFD results show a very good agreement with the experimental data.

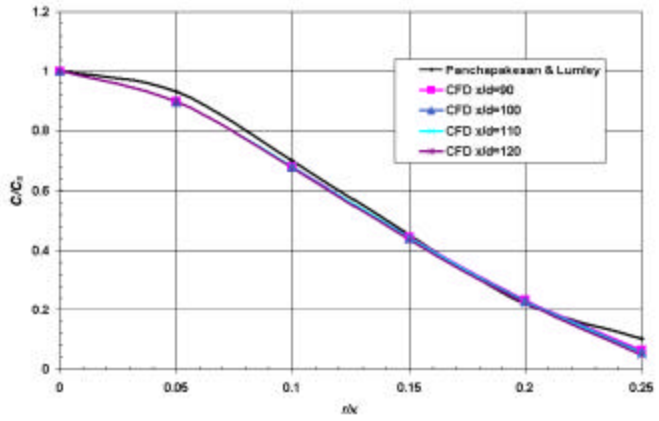

Figure 5. Radial profile of mean helium mass concentration

The dark blue line marks the correlated Panchapakesan and Lumley's data. The magenta, blue, cyan and purple lines mark the CFD results corresponding to x/d =90, 100, 110 and 120, respectively.

In order to further compare the CFD results with other experimental data obtained for vertical turbulent jets [1, 4], we consider the non-dimensionalization advocated by Chen and Rodi [6], which facilitates a unified representation of the experimental data (see also Panchapakesan and Lumley [5]).

Then nondimensional length (X_1), velocity (U_1) and concentration (g_1) can be defined as [5, 6]:

$$X_1 = F^{-\frac{1}{2}} w^{\frac{1}{4}} (x/d),\ U_1 = F^{\frac{1}{2}} w^{\frac{1}{4}} (U/U_j),\ g_1 = F^{\frac{1}{2}} w^{-\frac{3}{4}} a,$$

where F is the densimetric Froude number defined as $F = U_j^2 r_{He} / (r_{air} - r_{He}) gd$. In Panchapakesan and Lumley's experiments, the Froude number is equal to 1.4×10^4, or equivalent to the Richardson number of 7.14×10^{-5}. The Richardson number is generally defined as $Ri = \dfrac{(r_{air} - r_{He}) gd}{r_{He} U_j^2}$. (Here g = 9.81 m/s^2 is the gravity acceleration). Note that a is the helium volumetric concentration, which is also equal to $a = \dfrac{r_{air} - r}{r_{air} - r_{He}}$. The density ratio is $w = \dfrac{r_{air}}{r_{He}} = 7.24$.

Chen and Rodi, after reviewing existing experimental data, correlated the decay laws for velocity and concentration along the axis of the jet in the non-buoyant jet region (NBJ) and the buoyant plume region (BP) as [5, 6]:

$$U_1 = 6.2 w^{\frac{1}{2}} X_1^{-1},\ g_1 = 5.0 w^{-\frac{1}{2}} X_1^{-1}, \quad \text{for NBJ;} \tag{2}$$

$$U_1 = 3.5 w^{\frac{1}{3}} X_1^{-\frac{1}{3}},\ g_1 = 9.35 w^{-\frac{1}{3}} X_1^{-\frac{5}{3}}, \quad \text{for BP.} \tag{3}$$

Figure 6 shows the variation of the axial mean velocity in the non-dimensional coordinates suggested by Chen and Rodi. The CFD results from the coarse and fine meshes show a good agreement with Panchapakesan and Lumley's data, which is in the intermediate region (IR), and Chen and Rodi's correlations for NBJ and BP.

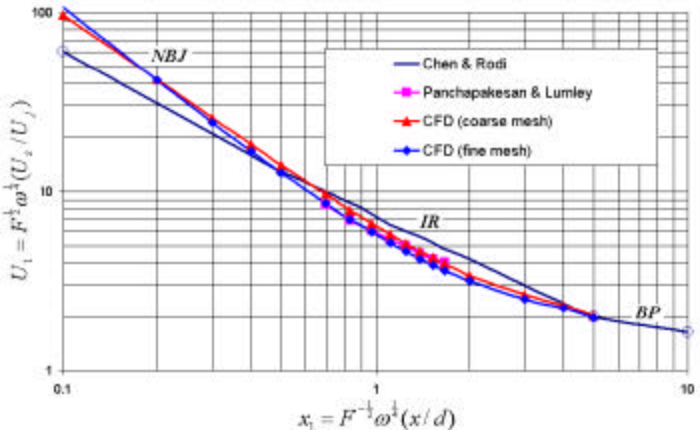

Figure 6. Variation of the axial mean velocity in the non-dimensional coordinates

The black line marks Chen and Rodi's correlation for the NBJ and BP regions. The magenta line marks Panchapakesan and Lumley's data. The red and blue lines are CFD results from the coarse (60×60) and the fine (90×90) meshes, respectively.

Figure 7 shows variation of the mean helium concentration (representing the buoyant force) in the non-dimensional coordinates. Various experimental data from Keagy and Weller [1], Way and Libby [2], Aihara et al. [3], Panchapakesan and Lumley [5] and the correlations from Chen and Rodi [6] were compared with the CFD results obtained on the coarse and fine meshes. The numerical results fit very well with Chen and Rodi's correlations and the experimental data.

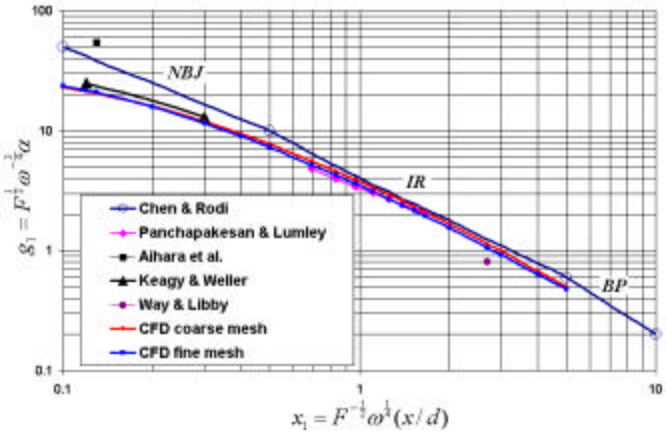

Figure 7. Variation of the mean helium concentration in the non-dimensional coordinates

The red and blue lines are CFD results from the coarse (60×60) and the fine (90×90) meshes, respectively. The data show a good agreement with the experimental data obtained by Panchapakesan and Lumley (Magenta, diamond), Aihara et al. (black, square), Keagy and Weller (black, triangle) and Way and Libby (purple, circle). The CFD data also fit very well with Chen and Rodi's correlations (dark blue, open circle).

4.0 CONCLUSION

In this validation research, a vertical helium jet reported by Panchapakesan and Lumley [5] was simulated using the CFD model based on the PHOENICS code. The real geometry was simplified by a 2-D axisymmetric computational domain to save the computational resources. The mixed gas was assumed to have incompressible gas properties so the inverse linear function was used to calculate the mixture density dependent on the local helium mass concentration and the helium and air densities. The PHOENICS software was used for solving the underlying incompressible Navier-Stokes equations, continuity equation and helium mass transport equation. The k-e RNG turbulence model, incorporated in the PHOENICS software, accurately predicted the velocity and mass/volumetric concentration profiles for the release with the errors less than 10%. The numerical results show a good agreement with experimental data of Panchapakesan and Lumley in both radial and axial directions. The simulation results were also compared with the published helium experimental data obtained by Keagy and Weller [1], Way and Libby [2], Aihara et al. [3] and the correlations made by Chen and Rodi [6] through the non-dimensionalization of length, velocity and concentration. The satisfactory agreement between the experimental and numerical data in the three jet regions proves that the current CFD model for gas release and dispersion is robust, accurate and reliable, and that the CFD technique can be used as an alternative to the experiments with similar helium jets. It also indicates that the CFD model can accurately predict similar hydrogen releases and dispersion if the model is correctly calibrated with hydrogen coefficients when applying to hydrogen jets.

ACKNOWLEDGEMENTS

The authors would like to thank Natural Resources Canada (NRCan) and Natural Sciences and Engineering Research Council of Canada (NSERC) for their contributions to funding of this work.

REFERENCES

1. Keagy, W. R. and Weller, A. E. “A study of freely expanding inhomogeneous jets”. Heat Transfer Fluid Mech Inst. X, 89-98, (1949).
2. Way, J. and Libby, P.A. “Hot-wire probes for measuring velocity and concentration in helium and air mixtures”. AIAA J. 8, 976-978 (1970).
3. Aihara, Y., Koyama, H. and Morishita, E. “Effects of an air stream on turbulent diffusion of helium jet from a small nozzle”. Phys. Fluids 17, 665-673 (1974).
4. Pitts, W. M. Effects of global density and Reynolds number variations on mixing in turbulent, axisymmetric jets. NBSIR 86-3340. National Bureau of Standards, US Department of Commerce.
5. Panchapakesan, N.R. and Lumley, J. L. “Turbulence measurements in axisymmetric jets of air and helium. Part 2. Helium jet”. J. Fluid Mech. Vol. 246, pp 225-247 (1993).
6. Chen, C. J and Rodi, W. “Vertical Turbulent Buoyant Jets – A review of Experimental Data”. HMT-4. Pergamon (1980).
7. Agranat, V., Cheng, Z. and Tchouvelev, A.V., “CFD Modeling of Hydrogen Releases and Dispersion in Hydrogen Energy Station”. 15th World Hydrogen Energy Conference, Yokahama, Japan, 27 June - 02 July (2004).
8. PHOENICS Hard-copy Documentation (Version 3.5). Concentration, Heat and Momentum Limited, London, UK, September 2002.
9. Yakhot, V., Orszag, S.A., Thangam, S., Gatski, T.B. and Speziale, C.G., “Development of turbulence models for shear flows by a double expansion technique”, Phys. Fluids A, 7, 1510, (1992).